



HAL
open science

5G vs Wifi6 downlink power consumption comparison for teleworking use case

Mohamed Yassine Hentati, Tijani Chahed, Philippe Ciblat, Marceau
Coupechoux, Sameh Najeh

► **To cite this version:**

Mohamed Yassine Hentati, Tijani Chahed, Philippe Ciblat, Marceau Coupechoux, Sameh Najeh. 5G vs Wifi6 downlink power consumption comparison for teleworking use case. 2023 IEEE Tenth International Conference on Communications and Networking (ComNet), Nov 2023, Hammamet, France. pp.1-9, 10.1109/ComNet60156.2023.10366633 . hal-04492334

HAL Id: hal-04492334

<https://hal.science/hal-04492334>

Submitted on 6 Mar 2024

HAL is a multi-disciplinary open access archive for the deposit and dissemination of scientific research documents, whether they are published or not. The documents may come from teaching and research institutions in France or abroad, or from public or private research centers.

L'archive ouverte pluridisciplinaire **HAL**, est destinée au dépôt et à la diffusion de documents scientifiques de niveau recherche, publiés ou non, émanant des établissements d'enseignement et de recherche français ou étrangers, des laboratoires publics ou privés.

5G vs Wifi6 Downlink Power Consumption Comparison for Teleworking Use Case

Mohamed Yassine Hentati⁽¹⁾, Tijani Chahed⁽²⁾, Philippe Ciblat⁽¹⁾, Marceau Coupechoux⁽¹⁾, Sameh Najeh⁽³⁾

⁽¹⁾ LTCI, Télécom Paris, Institut Polytechnique de Paris, France

⁽²⁾ SAMOVAR, Télécom SudParis, Institut Polytechnique de Paris, France

⁽³⁾ Sup'Com, Tunisia

Emails: mohamedyassine.hentati@supcom.tn; tijani.chahed@telecom-sudparis.eu; {philippe.ciblat, marceau.coupechoux}@telecom-paris.fr; sameh.najeh@supcom.tn

Abstract—Teleworking became a vastly popular practice lately owing to the Covid-19 outbreak. Our present study aims to evaluate the operating energy consumption in 5G versus Wifi6 networks for this remote working case study. We specifically study the detailed operations of transmission and reception at both radio access networks and quantify their power consumption in the downlink, analytically, using simulations and, for the case of Wifi6. We focus on three case studies in the framework of a teleworking tool: audio session, video session and shared screen session. Our results show that for the use case of video session in the downlink, when the number of users is rather small, Wifi6 consumes less power, however, as the number of users gets larger, 5G with Multi-User MIMO (MU-MIMO) outperforms the individual Wifi accesses. These results depend on the number of simultaneous MU-MIMO streams as well as on the fixed component of the power consumption of the 5G, for which we present a sensitivity analysis as well.

Index Terms—Power consumption, Wifi6 access point, 5G base station, downlink, teleworking.

I. INTRODUCTION

As the COVID-19 pandemic swept across the globe and social distancing was necessary to reduce contagion and spread, many governments strongly advocated or forced companies, schools and other organisations, to minimize physical presence at their premises, and to opt for teleworking [1]. This led a large number of businesses to turn to digital technologies to continue operating, with their employees working from home, using different tools such as videoconferencing, cloud services and virtual private networks. However, the type of digital (and especially wireless connection) technologies used for doing teleworking may have an influence on the power consumption of the whole network. Therefore this paper explores the power consumption of two

wireless technologies: Wifi6 and 5G for the cases of conferencing tools intensively used during teleworking: audio, video and screen sharing. Governmental policies in favor of a sustainable Information and Communication Technologies (ICT) or digital sobriety tend to favor Wifi against cellular technologies in their communication, see e.g. [2] in France. On the contrary, 5G has been presented as a key enabler for reducing our carbon footprint thanks for example to teleworking, see e.g. [3]. In fact, there are very few studies that really compare both technologies in terms of energy consumption. A first set of papers compares various wireless technologies in terms of energy consumption or energy efficiency. In [4] for example, authors compare the power consumption of 4G Long Term Evolution (LTE), WiMAX and 3G High Speed Data Access (HSPA). The work has been extended in [5] to include LTE-Advanced and various types of Base Stations (BS). The scope includes the home, access and core networks but the access network is the largest contributor. According to [5], LTE-Advanced, WiMAX and HSPA are ranked in this order in terms of covered area per watt. Authors insist on the importance of Multiple-Input-Multiple-Output (MIMO) to increase the energy efficiency. A comparison between WiFi and LTE is performed in [6] in the context of device-to-device communications. The conclusion states that LTE is less consuming when the number of users is relatively high, whereas WiFi is more energy efficient for small amount of data. This part of the literature however does not include Wifi6 nor 5G. A second set of papers specifically compare Wifi6 and 5G. For example, Naik et al. in [7], [8] identify current challenges in unlicensed bands and compare Wifi6 and 5G New Radio (NR) but ignore the energy consumption aspect. Maldonado et al. [9] compare Wifi6 and 5G in an industrial Internet

of things context. They however focus on latency and reliability and omit the energy consumption. To the best of our knowledge, Wifi6 and 5G have never been compared in terms of energy consumption. Only few works compare the energy consumption of several access technologies for a given use case. In [10] for instance, the authors compare energy consumption of Bluetooth Low Energy (BLE) versus Wifi in the context of smart buildings. Bluetooth is shown to be about 30% more energy efficient than Wifi in occupancy data transmission from user's smartphone to the communication end points. In [11], authors compare WiFi and LTE power consumption for video streaming using on-site measurements. Overall, Wifi is shown to be more energy efficient and to consume also less power. The influence of the number of users is however only partly tackled, a detailed study of the capacity of the LTE cell would have been required. Again, to the best of our knowledge, there is no specific energy consumption comparison between wireless technologies for the teleworking use case.

Our work also differs from classical studies on the carbon impact of video streaming. In [12] for example, the scope is rather a macroscopic view of the whole system, including the terminal, the network and the data center. Moreover, the approach is *attributional* in the sense that a certain share of the whole system impact is attributed to one video. It relies on global energy intensity estimates. On the contrary, we propose a microscopic analysis focusing on a detailed view of the access points and base stations allowing us to consider all operations of these equipment, both when active and idle. This enables us in turn to model the load of the network, the corresponding system dimensioning and quantify the overall power consumption.

In this work, we thus compare the energy consumption of 5G versus Wifi6 for the use case of teleworking. We consider K users involved in a conferencing session (screen sharing, video, or audio). We assume without loss of generality that every user is involved in a single session composed of a single, symmetrical flow. These users can be either jointly served by a single 5G Base Station (BS) or individually by different Wifi6 Access Points (AP) as drawn in Figure 1. In the Wifi6 scenario, every user is served by a single AP and every AP serves a single user. Therefore we have K APs. We compare both scenarios in terms of the downlink operational power consumption of the serving equipment (either the BS or the APs). We focus on the downlink at the serving network equipment since its power amplifier is not used during the uplink phase. We do not consider the wired

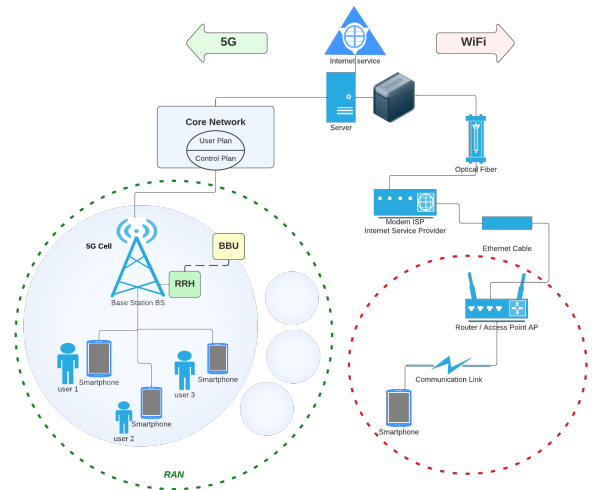


Fig. 1: Network Models for 5G and Wifi6.

backhaul and core network of the operator, as they are supposed to have comparable power consumption in both cases. We do not also consider the terminals, assuming that they are identical in both scenarios. At last, we exclude the power consumption required for the manufacturing of the equipment and their end-of-life.

Our contributions are as follows

- We analyze the different steps for the transmission and reception at the radio level for Wifi6 and 5G and derive analytical formulations for the power consumption of both access technologies based on their respective parameters as well as those of the considered session.
- We provide numerical evaluations for the energy consumption thanks to the models obtained in the first item. We compare them to some values previously available in the literature coming from the operators.
- We compare the values obtained for both access technologies and provide the threshold on K for which one system is more advantageous than the other in terms of operational power consumption.

The remainder of this paper is organized as follows: in Section II, we provide the power consumption model for the Wifi6 in the downlink. In Section III, we analyze the power consumption model for 5G for the case of a distributed BS. In Section IV, we numerically illustrate the power consumption for both systems under practical assumptions. Eventually comparison between both systems are carried out. Section V is devoted to concluding remarks.

II. POWER CONSUMPTION IN WIFI6

We first evaluate the energy consumed by a Wifi6 AP. The IEEE standard for the lower layers of Wifi6 is called IEEE802.11ax. We consider the downlink while assuming a single user involved in a constant bit rate video session. We assume that the teleworking application periodically generates packets of length L at a rate D . Consequently, the delivery time we need to satisfy is

$$T_{\text{delivery}} = \frac{L}{D}. \quad (1)$$

This time corresponds to a cycle which we repeat until the queue is empty, i.e. the application session is over. In the rest of the section, we describe the different steps involved in the packet transmission along with their duration and energy consumption.

A. Physical layer

The IEEE 802.11ax standard is based on Orthogonal Frequency Division Multiple Access (OFDMA) [13]. The bandwidth is divided into tones (or subcarriers) which are grouped into Resource Units (RU) (or subchannels). The number of subcarriers per RU, the location of the RUs in the band and the number of RUs depend on the channel configuration and bandwidth. Let T_u denote the duration of the OFDM symbol useful part, and T_g the duration of the Guard Interval. The total symbol duration is given by $T = T_u + T_g$. The Guard Interval duration can be configured, however, we choose the smallest value since it is well adapted for indoor, where teleworking usually takes place.

The number of bits transmitted during one OFDM symbol depends on the number of data subcarriers (denoted by N_s) and the number of bits per subcarrier. The latter is equal to $r \log_2(M)$ where M is the constellation size and r the channel coding rate. For the sake of simplicity, we assume that the Modulation and Coding Scheme (MCS) is identical for all subcarriers. We may also have more than one spatial stream due to MIMO which we denote by N_{ss} . Therefore, the physical data rate R is as follows:

$$R = \left(\frac{N_s \times r \times \log_2(M)}{T} \right) \times N_{ss}, \quad (2)$$

B. Frame structure

In IEEE 802.11ax, a frame is called High Efficiency Physical layer Protocol Data Unit (HE PPDU). There are four different frame structures but in our single user case, the so-called HE SU PPDU applies (SU stands for Single User). Each PPDU starts with a preamble providing

useful information on the physical layer: for instance, the bandwidth, the RU allocation and the chosen MCS. The preamble of the HE SU PPDU is composed of an invariant part of duration T_{inv} , a Packet Extension (PE) field of duration T_{pe} which will be set to 0 in this paper, and a Channel estimation field, termed HE Long Training Field (HE-LTF), of duration $T_{\text{he-ltf}}$, which is repeated as many times as there are MIMO spatial streams. Consequently, the transmission time for the preamble of such a PPDU is

$$T_{\text{preamble}} = T_{\text{inv}} + T_{\text{pe}} + N_{ss} \times T_{\text{he-ltf}}. \quad (3)$$

Taken into account the frame load, the transmission time T_P of the packet sent by the application is thus:

$$T_P = T_{\text{preamble}} + \frac{L}{R}. \quad (4)$$

When a terminal (or STA standing for station) receives a HE SU PPDU, it shall respond with an HE SU PPDU which is either an ACK frame, a QoS Data frame or a multi-STA BlockAck. In the simplest case, it is an ACK frame. The preamble of the ACK is the same as for the data frame. The information in this ACK frame is coded over L_{ACK} bits. Assuming that the same MCS is used for the data and for the ACK frame, the transmission time for the ACK is:

$$T_{\text{ACK}} = T_{\text{preamble}} + \frac{L_{\text{ACK}}}{R}. \quad (5)$$

C. Downlink frame exchange

We assume that the AP wants to transmit a packet of the teleworking application to the STA.

- First, the AP uses the classical CSMA/CA procedure to access the channel. This procedure is based on channel sensing, a back-off mechanism and on the division of time into mini-slots (also called slots in the rest of the paper). As there is a single STA in our case, there is no need for a Ready To Send (RTS) and Clear To Send (CTS) exchange before transmitting a data frame. The average time required to access the channel is denoted by T_{acc} . In the absence of competition on the medium, we assume that the contention window is set to its minimum value CW_{min} . As the backoff mechanism chooses its value uniformly in the interval $[1, CW_{\text{min}}]$, we have:

$$T_{\text{acc}} = \frac{CW_{\text{min}}}{2} T_{\text{slot}}, \quad (6)$$

where T_{slot} is the time slot duration for this step.

- Then, the AP transmits the frame, which is a HE SU PPDU, to the STA using the assigned RUs and the

chosen MCS. For a single STA, the whole channel bandwidth is used for the transmission, and the transmission duration is given by (4).

- If the frame is received successfully, the STA responds after a Short Inter-Frame Space (SIFS) of duration T_{sifs} with an ACK frame in its assigned RUs. We assume that frames are always received with success and thus that there is no retransmissions. This represents a best case in terms of energy consumption.
- Once the AP receives the ACK, there is a residual time of duration T_{res} until the end of the cycle, see (1). During this residual time, there is no frame exchange. The residual duration is deduced from other durations by:

$$T_{\text{res}} = T_{\text{delivery}} - (T_{\text{acc}} + T_P + T_{\text{sifs}} + T_{\text{ACK}}). \quad (7)$$

In this frame exchange process, we have neglected the transmission of management frames.

D. Wifi6 operational power consumption

Summarizing all the steps of the downlink transmission, the power consumption is given as follows:

$$P = \frac{E}{T_{\text{delivery}}} \quad (8)$$

where $E = E_{\text{acc}} + E_P + E_{\text{sifs}} + E_{\text{ACK}} + E_{\text{res}}$, with

$$E_{\text{acc}} = T_{\text{acc}} \times P_{\text{idle}}, \quad (9)$$

$$E_P = T_P \times P_{\text{TX}}, \quad (10)$$

$$E_{\text{sifs}} = T_{\text{sifs}} \times P_{\text{idle}}, \quad (11)$$

$$E_{\text{ACK}} = T_{\text{ACK}} \times P_{\text{RX}}, \quad (12)$$

$$E_{\text{res}} = T_{\text{res}} \times P_{\text{idle}}. \quad (13)$$

are the energy consumption terms corresponding to every step of the transmission. The terms P_{idle} , P_{TX} and P_{RX} correspond to the powers consumed by the AP in the idle, transmit and receive states, respectively. We denote by $E_{\text{ld}} = E_P + E_{\text{ACK}}$ the load-dependent component of the consumed energy. We have considered here that the carrier sensing process performed during access and residual time is equivalent to an idle state in terms of energy consumption.

III. POWER CONSUMPTION IN 5G

A. Physical data rate with MU-MIMO

We now consider 5G, where the first step is to find the relationship between the data rate and the number of users we can serve simultaneously within a cell.

We recall that 5G uses the Multi-User Multiple Input-Multiple Output (MU-MIMO) technology and we rely on [14] to determine the capacity of a 5G cell. In this reference, authors assume that every user has a single antenna whereas the BS is equipped with N_a antennas. If the users are requiring the same physical data rate, they should experience the same Signal-to-Interference Ratio (SIR). Note that noise can be neglected here in an interference limited environment like an urban area. Co-channel interference is due to the presence of neighboring cells adopting the same carrier frequency. Equal SIR at the users is then obtained by an adequate channel-dependent power allocation.

With N_a antennas, the BS can simultaneously serve up to N_a users with MU-MIMO. If it simultaneously serves $K_u \leq N_a$ users, the physical data rate for each user can be written as [14]:

$$\underline{R} = B \log_2 \left(1 + \frac{N_a/K_u}{1 + \frac{1}{K_u} \sum_{k=0}^{K_u-1} 1/\rho_k} \right) \quad (14)$$

where B is the bandwidth; ρ_k is the local average SIR of user k in the cell of interest, which is given by:

$$\rho_k = \frac{G_k}{\sum_{\ell \neq 0} G_{\ell,k}} \quad (15)$$

G_k and $G_{\ell,k}$ are the large scale gains between user k and the BS of interest and BS ℓ , respectively.

Where, the K_u users are uniformly distributed within a cell, the average user data rate R is given as

$$R = B \log_2(e) \int_0^\infty \frac{1 - e^{-z}}{{}_1F_1(1, 1 - 2/\eta, z/N_a)^{K_u}} \frac{dz}{z} \quad (16)$$

where ${}_1F_1$ is the confluent hypergeometric function and η is the path loss [14].

B. Number of multiplexed users

Recall now that the BS sends a single packet to each user every T_{delivery} , see (1). In this time interval, the BS has thus the possibility to multiplex several teleworking applications in a time-sharing fashion and using MU-MIMO. During an interval of length T_{delivery} , we thus assume that the BS serve K users in total. As the BS can serve at most N_a users simultaneously by MU-MIMO, we decompose K as follows: $K = S.N_a + K_r$ with $K_r < N_a$. Consequently within the delivery duration, we have S periods which are “full”, i.e., $K_u = N_a$, and one period which is “not-full” with $K_u = K_r$.

The data rate per user for the “full” period is R_f given by (16) by setting $K_u = N_a$. The “non-full” period

enables a data rate per user R_{nf} given by (16) by setting $K_u = K_r$.

Then the full period duration is $T_f = L/R_f$, and the non-full period is $T_{nf} = L/R_{nf}\mathbf{1}_{K_r>0}$, where $\mathbf{1}_{K_r>0} = 1$ when $K_r > 0$ and 0 otherwise. Obviously, the value K is achievable if and only if

$$ST_f + T_{nf} \leq \alpha T_{\text{delivery}},$$

where α is the proportion of time devoted to the down-link, assuming a Time Division Duplex (TDD) mode in 5G, or equivalently:

$$S/R_f + 1/R_{nf} \leq \frac{\alpha}{D}. \quad (17)$$

We denote by K_{\max} the maximum value of K that the cell can serve within an interval of duration T_{delivery} .

C. 5G operational power consumption

We are now ready to evaluate the power consumption of a 5G cell. For that, we consider the model developed by [15] in the massive MIMO case. Actually, we consider the mapping:

$$K_u \mapsto Q_{K_u} = \frac{P_{\max}}{\eta_{PA}} + P_{\text{li}} + D_0 N_a + C_3 K_u^3 \quad (18)$$

$$+ D_1 N_a K_u + D_2 N_a K_u^2 + P_b K_u R$$

where K_u is the number of simultaneously multiplexed users with MU-MIMO at the BS, and R is the user data rate. Moreover, P_{\max} is the transmission power of the BS, η_{PA} is the Power Amplifier (PA) power efficiency, P_{li} is the load-independent power consumption, D_0 is the power consumed by the transceiver module associated with each antenna. The terms starting with C_3 , D_1 , and D_2 are related to different parts of the beamforming processing and the channel estimation step. The term associated with P_b takes into account the coding/decoding step. We assume that the BS transmits at maximum total power when it is active.

We are now able to express the BS consumption during an interval of duration T_{delivery} . The energy used during this interval is:

$$E = S \times Q_{N_a} T_f + Q_{K_r} T_{nf} + P_{\text{li}} T_{\text{idle}} \quad (19)$$

where $T_{\text{idle}} = T_{\text{delivery}} - ST_f - T_{nf}$, which leads to the following equation used in the remainder of the paper:

$$P = \frac{S \times Q_{N_a} T_f + Q_{K_r} T_{nf} + P_{\text{li}} T_{\text{idle}}}{T_{\text{delivery}}} \quad (20)$$

with S and K_r satisfying (17).

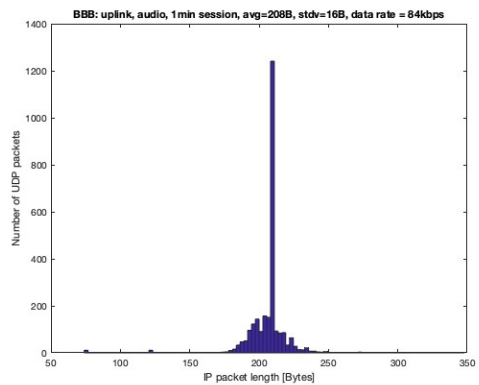


Fig. 2: Audio packet size distribution.

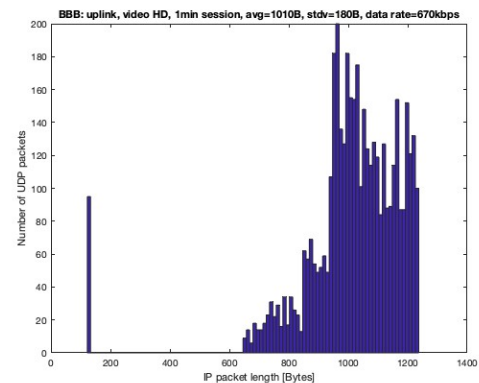


Fig. 3: Video packet size distribution.

IV. NUMERICAL EVALUATIONS

A. Packet size estimation

Via the software Wireshark¹, we can plot the packet size distribution between two users communicating between each other. In Figs. 2, 3, and 4, we display the packet size distribution for the audio session, the video session, and the screen sharing session, respectively. The application data rate for each session appears in the title of each corresponding figure. These histograms have been obtained by scanning one minute of the conferencing application BigBlueButton². Distributions have been obtained on the uplink for ease of implementation but the traffic is supposed to be symmetric.

We observe that:

- For an audio session, the packet size is relatively small. We consider the average value $L = 208$ bytes,

¹Wireshark is a network packet analyzer [16].

²BigBlueButton is an open source virtual classroom software used for web conference and e-learning [17].

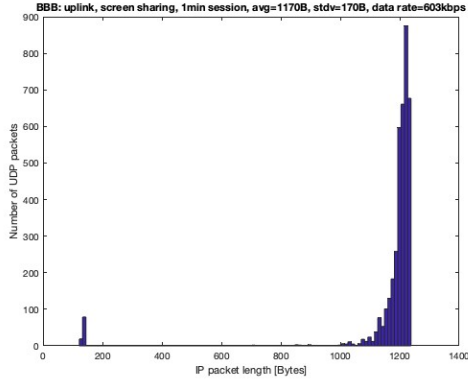


Fig. 4: Shared screen packet size distribution.

Parameter	Value
T_u	$12.8\mu\text{s}$
T_g	$0.8\mu\text{s}$
N_s	234 (20MHz), 980 (80MHz)
r	$3/4$
M	16
N_{ss}	2
T_{inv}	$36\mu\text{s}$
T_{pe}	$0\mu\text{s}$
T_{he-ltf}	$7.2\mu\text{s}$
L_{ACK}	112bits
CW_{min}	15
T_{slot}	$9\mu\text{s}$
T_{sifs}	$10\mu\text{s}$

TABLE I: Wifi6 parameters.

- For a video session, the packet size is much larger and the variance is larger. For numerical applications, we will consider $L = 1010$ bytes,
- For a shared screen session, the packet size is often close to the maximum value allowed by the protocol (1200 bytes). We will consider $L = 1170$ bytes.
- The data rates D for audio, video and screen sharing sessions are equal to 84kbits/s, 670kbits/s, and 603kbits/s, respectively.

B. Wifi6 numerical results

The parameters associated with Wifi6 have been reported in Table I. We have chosen a MCS with a medium spectral efficiency of 3bit/s/Hz per link. To compute (9)-(13), we use the values of P_{TX} , P_{RX} , and P_{idle} given in Table II for two recent APs from two French operators. P_{TX} and P_{idle} have been obtained from the respective public data of the operators, while P_{RX} has been extrapolated.

We are now able to compute the power consumption for the three types of sessions described in Section IV-A.

AP name	P_{TX}	P_{RX}	P_{idle}
AP1 (Bbox Ulym - Wifi6)	11W	9.5W	8W
AP2 (Orange Livebox - Wifi6)	15.3W	11.5W	7.8W

TABLE II: Transmission parameters for different APs.

AP s name	Bandwidth	E_{ld}	E	P
AP1	20MHz	1.220mJ	158.752mJ	8.013W
	80MHz	1.077mJ	158.714mJ	8.012W
AP2	20MHz	1.609mJ	155.112mJ	7.83W
	80MHz	1.412mJ	155.108mJ	7.82W

TABLE III: Energy and power consumptions for an audio session with different APs.

AP name	Bandwidth	E_{ld}	E	P
AP1	20MHz	1.904mJ	96.940mJ	8.038W
	80MHz	1.241mJ	96.755mJ	8.023W
AP2	20MHz	2.560mJ	95.221mJ	7.89W
	80MHz	1.639mJ	94.765mJ	7.85W

TABLE IV: Energy and power consumptions for video session with different APs.

APs name	Bandwidth	E_{ld}	E	P
AP1	20MHz	2.040mJ	124.139mJ	7.99W
	80MHz	1.273mJ	123.963mJ	7.98W
AP2	20MHz	2.750mJ	122.323mJ	7.88W
	80MHz	1.680mJ	121.802mJ	7.84W

TABLE V: Energy and power consumptions for screen sharing session with different APs.

In Tables III, IV and V, we show the energy consumption for one packet and the power consumption for an audio, a video and a screen sharing session, respectively. We observe that the power consumptions for the three cases are not dramatically different with respect to the types of sessions and the bandwidth; the screen sharing session is a little bit more greedy in terms of power consumption. This is explained by the fact that power consumption is dominated by the idle period which is the same across the three cases. Indeed, the term E_{ld} is very small compared to the total energy.

C. 5G numerical results

The parameters associated with 5G have been reported in Table VI and have been taken from [15]. All the power consumption evaluations have been obtained through (20). We plot in Fig. 5 the power consumption versus the number of users K for different numbers of antennas N_a at the BS. As expected, the number of multiplexed users K increases with the number of antennas N_a at the BS. Each curve stops at the value of K_{max} that is given by (17), and which, as stated

Parameter	value
η_{PA}	0.39
P_{\max}	220W
P_{li}	20W
C_3	10^{-7} W
D_0	1W
D_1	0.003W
D_2	9.4×10^{-7} W
P_b	1.15W/(Gbits/s)
B	80MHz
α	2/3
η	4

TABLE VI: 5G parameters.

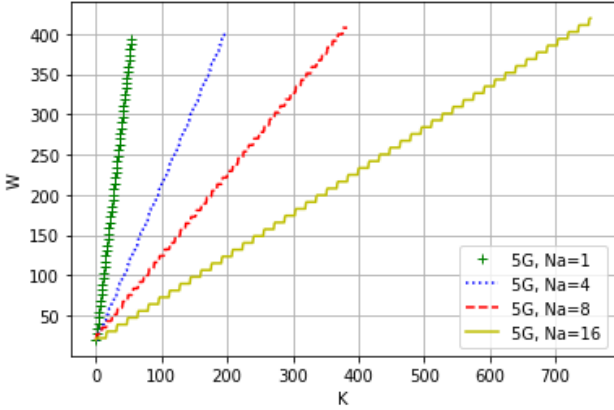


Fig. 5: Power consumption versus $K \in \{1, \dots, K_{\max}\}$ for different number of antennas N_a .

earlier, increases with N_a . This shows the advantage of MU-MIMO. All curves however reach approximately the same maximum power, as the power budget is the same in all cases for a fair comparison.

D. Comparison between Wifi6 and 5G

We now compare the energy consumption for Wifi6 and 5G when a BBB video session is run (assuming thus a data rate of $D = 670$ kbits/s and a packet size of $L = 1010$ bytes). We plot in Fig. 6 the power consumption versus the number of users K for Wifi6 with the two APs mentioned in Table II and for 5G with different values of number of antennas N_a . Note that for the 5G curves, Fig. 6 is just a zoom on Fig. 5 around small values of K , i.e., we focus on the range from 0 to less than 30 users for all values of N_a . We observe that, for $N_a = 1$, when $K < 16$ for AP₁ and when $K < 20$ for AP₂, the set Wifi6 consumes less power than 5G for a video session; for higher values of K , 5G consumes less power. For values of N_a equal to 4, 8 and 16, the intersection takes place at lower values of K , around 3 video users. In this

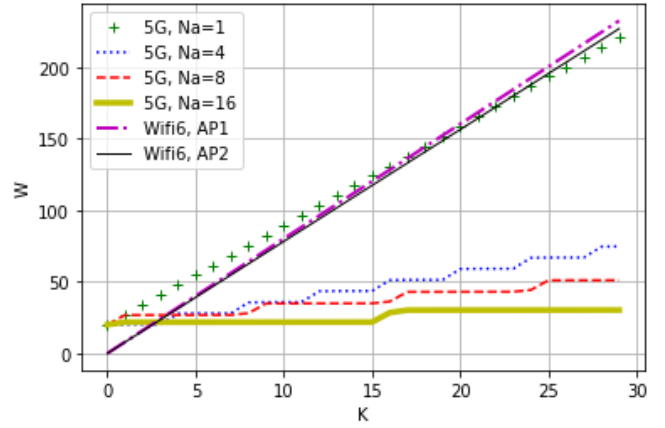


Fig. 6: Total power consumption versus K for Wifi6 and 5G (zoom on Fig. 5 for 5G curves).

figure 6, the chosen value of P_{li} , taken from [15], is quite small compared to other values found in the literature. However, by taking the value provided in [18] which corresponds to half the power consumed at full load, we obtain the results shown in Fig. 7 (in the range from 0 to 100 users for all values of N_a). We observe that the crossing point is higher than in the previous case shown in Fig. 6, between 50 and 65 users for N_a equal to 4, 8 and 16. For $N_a = 1$, 5G always consumes more energy than Wifi6, up to the maximum 5G capacity of 54 users in the cell. This shows the importance of the MU-MIMO transmission scheme in 5G.

For the cases of audio session and screen sharing (not shown here), the intersections between 5G power consumption (using 8 antennas and the larger load-independent power consumption) and Wifi6 using AP1 and AP2 are around 50 and 55 users, respectively, close to the case of video session (intersection at 58).

V. CONCLUSION

In this paper, we analyze the power consumption of Wifi6 and 5G when using teleworking applications such as video, audio and screen sharing sessions. We observe that 5G is quite efficient as soon as the number of users is large enough, although this number strongly depends on the value of the load-independent component of the power model. We show that MU-MIMO in 5G plays a deciding role in the comparison with Wifi6. This work could be extended along the following potential directions: i) 5G may propagate poorly indoor and this drawback has not been taken into account, ii) the energy consumption for manufacturing the systems has not been taken into account while 5G is being installed whereas

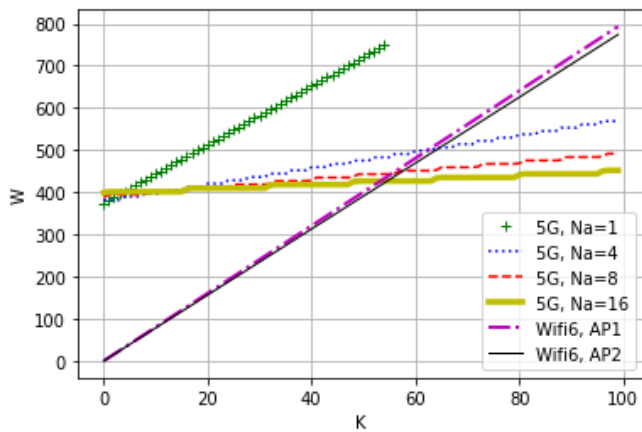


Fig. 7: Total power consumption versus K for Wifi6 and 5G with larger fixed power component for 5G than in Fig. 6.

Wifi6 is already largely deployed, iii) in order to limit the number of APs and amortize the idle phase in Wifi6, sharing the AP amongst users should be also taken into account and advocated, iv) Wifi6 is not cheap in energy due to the fixed power consumed during idle phase. Therefore sleep mode policy for Wifi6 has to be more aggressive and activated more often at the expense of additional but acceptable delay when application is started. A comparison is then required with 5G implementing so-called Advanced Sleep Modes (ASM) [19], and v) extending this methodology for other applications such as video on demand.

VI. ACKNOWLEDGEMENT

This research was produced within the framework of Energy4Climate Interdisciplinary Center (E4C) of IP Paris and Ecole des Ponts ParisTech. This research was supported by 3rd Programme d'Investissements d'Avenir [ANR-18-EUR-0006-02].

REFERENCES

- [1] A. Hook, B. K. Sovacool, S. Sorrell *et al.*, "A systematic review of the energy and climate impacts of teleworking," 2020.
- [2] "10 bons gestes numériques en télétravail," <https://agirpourlatransition.ademe.fr/particuliers/bureau/numerique/10-bons-gestes-numeriques-teletravail>, accessed: 2023-02-13.
- [3] J. Bieser, B. Salieri, R. Hischier, and L. Hilty, "Next generation mobile networks: Problem or opportunity for climate protection?" 2020.
- [4] M. Deruyck, W. Vereecken, E. Tanghe, W. Joseph, M. Pickavet, L. Martens, and P. Demeester, "Comparison of power consumption of mobile wimax, hspa and lte access networks," in *2010 9th Conference of Telecommunication, Media and Internet*, 2010, pp. 1–7.
- [5] Deruyck, Margot and Vereecken, Willem and Joseph, Wout and Lannoo, Bart and Pickavet, Mario and Martens, Luc, "Reducing the power consumption in wireless access networks: overview and recommendations," *Progress in Electromagnetics research-pier*, vol. 132, pp. 255–274, 2012. [Online]. Available: <http://dx.doi.org/10.2528/PIER12061301>
- [6] M. Condoluci, L. Militano, A. Orsino, J. Alonso-Zarate, and G. Araniti, "Lte-direct vs. wifi-direct for machine-type communications over lte-a systems," in *2015 IEEE 26th Annual International Symposium on Personal, Indoor, and Mobile Radio Communications (PIMRC)*, 2015, pp. 2298–2302.
- [7] G. Naik, J.-M. Park, J. Ashdown, and W. Lehr, "Next generation wi-fi and 5g nr-u in the 6 ghz bands: Opportunities and challenges," *IEEE Access*, vol. 8, pp. 153 027–153 056, 2020.
- [8] G. Naik and J.-M. J. Park, "Coexistence of wi-fi 6e and 5g nr-u: Can we do better in the 6 ghz bands?" in *IEEE INFOCOM 2021 - IEEE Conference on Computer Communications*, 2021, pp. 1–10.
- [9] R. Maldonado, A. Karstensen, G. Pocovi, A. A. Esswie, C. Rosa, O. Alanen, M. Kasslin, and T. Kolding, "Comparing wi-fi 6 and 5g downlink performance for industrial iot," *IEEE Access*, vol. 9, pp. 86 928–86 937, 2021.
- [10] G. D. Putra, A. R. Pratama, A. Lazovik, and M. Aiello, "Comparison of energy consumption in wi-fi and bluetooth communication in a smart building," in *2017 IEEE 7th Annual Computing and Communication Workshop and Conference (CCWC)*, 2017, pp. 1–6.
- [11] L. Zou, A. Javed, and G.-M. Muntean, "Smart mobile device power consumption measurement for video streaming in wireless environments: Wifi vs. lte," in *2017 IEEE International Symposium on Broadband Multimedia Systems and Broadcasting (BMSB)*, 2017, pp. 1–6.
- [12] C. Trust, "Carbon impact of video streaming," <https://www.carbontrust.com/our-work-and-impact/guides-reports-and-tools/carbon-impact-of-video-streaming>, June 2021, accessed: 2023-06-22.
- [13] "Ieee standard for information technology–telecommunications and information exchange between systems local and metropolitan area networks–specific requirements part 11: Wireless lan medium access control (mac) and physical layer (phy) specifications amendment 1: Enhancements for high-efficiency wlan," *IEEE Std 802.11ax-2021 (Amendment to IEEE Std 802.11-2020)*, pp. 1–767, 2021.
- [14] G. George, A. Lozano, and M. Haenggi, "Massive mimo forward link analysis for cellular networks," *IEEE Transactions on Wireless Communications*, vol. 18, no. 6, pp. 2964–2976, 2019.
- [15] D. López-Pérez, A. D. Domenico, N. Piovesan, X. Geng, H. Bao, Q. Song, and M. Debbah, "A survey on 5g radio access network energy efficiency: Massive mimo, lean carrier design, sleep modes, and machine learning," *IEEE Commun. Surv. Tutorials*, vol. 24, no. 1, pp. 653–697, 2022. [Online]. Available: <https://doi.org/10.1109/COMST.2022.3142532>
- [16] U. Lamping and E. Warnicke, "Wireshark user's guide," *Interface*, vol. 4, no. 6, p. 1, 2004.
- [17] C. Ukoha, "As simple as pressing a button? a review of the literature on bigbluebutton," *Procedia Computer Science*, vol. 197, pp. 503–511, 2022.
- [18] G. Auer, V. Giannini, C. Desset, I. Godor, P. Skillermark, M. Olsson, M. A. Imran, D. Sabella, M. J. Gonzalez, O. Blume, and A. Fehske, "How much energy is needed to run a wireless network?" *IEEE Wireless Communications*, vol. 18, no. 5, pp. 40–49, 2011.

- [19] F. E. Salem, T. Chahed, E. Altman, A. Gati, and Z. Altman, "Optimal policies of advanced sleep modes for energy-efficient 5g networks," in *18th IEEE International Symposium on Network Computing and Applications, NCA 2019, Cambridge, MA, USA, September 26-28, 2019*, A. Gkoulalas-Divanis, M. Marchetti, and D. R. Avresky, Eds. IEEE, 2019, pp. 1–7.